Chinese Journal of Electronics
vol. 33, no. 2, pp. 504–515, March 2024
https://doi.org/10.23919/cje.2022.00.113

RESEARCH ARTICLE

Blind Signal Reception in Downlink Generalized Spatial Modulation Multiuser MIMO System Based on Minimum Output Energy

Wei-Chiang WU

College of Mechanical and Electrical Engineering, Sanming University, Sanming 365004, China

Corresponding author: Wei-Chiang WU, Email: lclunds@163.com
Manuscript Received May 3, 2022; Accepted October 8, 2022

Abstract — This paper considers downlink multiuser multiple-input-multiple-output system with parallel spatial modulation scheme, in which base station transmitter antennas are separated into K groups corresponding to K user terminals. Generalized spatial modulation is employed, in which a subset (more than single antenna) of transmit antenna array are activated and the activating pattern corresponds to specific spatial symbol. Different from existing precoding-based algorithms, we develop a two-stage detection scheme at each user terminal: In the pre-processing stage, a minimax algorithm is proposed to identify the indices of active antennas, where the key idea is that the minimum output energy of the detector is maximized; A constrained minimum output energy algorithm is proposed in the post-processing stage to mitigate multiuser interference and extract temporal symbols. Compared with existing precoding-based algorithms, the complexity is significantly reduced. Moreover, the proposed algorithm is semi-blind, in which only a small subset of channel state information is required to identify active antennas as well as eliminate multiuser interference. Simulation results demonstrate that the proposed algorithm is near-far resistant and the spectral efficiency is extensively increased compared to the conventional spatial modulation scheme.
Keywords — Generalized spatial modulation, Multiuser multiple-input-multiple-output, Multiuser interference , Minimum output energy, Minimax.
Citation — Wei-Chiang WU, "Blind Signal Reception in Downlink Generalized Spatial Modulation Multiuser MIMO System Based on Minimum Output Energy," *Chinese Journal of Electronics*, vol. 33, no. 2, pp. 504–515, 2024. doi: 10.23919/cje.2022.00.113.

I. Introduction

Recently, spatial modulation (SM) technique has received much attention [1]–[5] since it uses the index in an antenna array system to convey extra information such that the throughput is increased. In SM scheme, the transmitted bits are separated into two information-carrying symbols: One block of bits is mapped to the conventional signal constellation diagram (temporal symbol), e.g., M-ary phase shift keying (PSK) symbol. While the other block of information bits (spatial symbol) determines the activated antenna index at the transmitter for temporal data transmission. It has also been shown in [6]–[8] that SM technique is an attractive modulation and transmission technique in multiple-input-multiple-output (MIMO) systems with reduced complexity since only single radio frequency (RF) chain is required at each time slot. There have been some attempts in [9]–[13] to realize SM-based uplink multiuser (MU)-MIMO systems. In [9], a maximum likelihood (ML) receiver is implemented to demodulate the two-user symbols in uplink SM MU-MIMO scheme, whereas, the complexity of the ML detector expands vastly as the number of users increases. Then, some suboptimum algorithms are proposed: The message passing-based multiuser receiver has been proposed in [10]. The nearest neighbor search (NNS) algorithm is developed in [11] to find the active antenna indices. The work of [12] uses the space-alternating generalized expectation maximization (SAGE) algorithm and successive interference cancellation (SIC) method that iteratively demodulate desired user's data while remove the multiuser interference (MUI) from undesired users. The SAGE-aided list projection (S-LP) multiuser SM receiver is proposed in [13].

Associate Editor: Prof. Ran TAO, Beijing Institute of Technology.

The use of SM for downlink (DL) MU-MIMO transmission has also been investigated in [14]–[23]. In general, the SM DL MU-MIMO system can be categorized into two different schemes: The scheme considered in [14]–[18] termed as receive SM (RSM) employs zero-forcing (ZF) precoding aided SM technique at the base station transmitter (BSTx) to activate single receive antenna at each user terminal (UT). The second scheme considered in [19]–[21] termed as parallel SM (PSM) separates the BSTx antennas into K groups corresponding to K UTs. In what follows, different disjoint sets of antennas are dedicated to different UT such that each set is considered for point-to-point SM transmission of a particular UT. In other words, the DL MU SM transmission is composed of K parallel single user SM transmissions. Specifically, a novel antennas management and selection method named spatial modulation multiple access (SMMA) is proposed in [19] that adaptively allocate the BSTx antennas to multiple users to increase capacity in MU SM. Alternatively, references [22]–[24] exploit block diagonalization (BD) precoding aided SM technique to realize quadrature SM (QSM)-based DL MU-MIMO system. Because of multiple antennas are activated at the same time instant, each UT is contaminated by MUI emitted from the antennas assigned to other users. All the above works exploit the full channel state information (CSI) at the BSTx to design the ZF or BD precoder. Since the MUI is completely eliminated, thus single user detector can be employed at each UT. In a nutshell, the disadvantages of existing works related to SM DL MU-MIMO includes:

1) ZF or BD precoder employs full CSI at the BSTx to completely eliminate MUI. This requirement is impractical in massive MIMO system, where massive amount of CSI needs to be estimated and updated. Moreover, it is inevitable for CSI perturbation since wireless channel is time-varying and channel reciprocity is not satisfied in FDD system. This leads to disastrous performance degradation since ZF precoder can hardly eliminate MUI.

2) All the BSTx antennas are activated in the RSM scheme, leading to massive RF chains. This induces higher complexity transmitter structure compared to conventional SM scheme.

3) The restriction for DL MU-MIMO systems based on ZF precoding is that the number of BSTx antennas should be larger than the sum of all UT antennas, i.e., it requires that $N_{\text{tot}} \geq K \times N_r$, where N_{tot}, K, N_r denotes the numbers of BSTx antennas, UTs, and UT antennas, respectively. While in BD precoding scheme, the restriction is $N_{\text{tot}} = K \times N_r$. This is hard to attain especially in current and future network with a massive number of UTs. Moreover, it is inflexible in the network with dynamic number of UTs, i.e., additional users are not easy to be included or removed to the system.

4) As will be analyzed in Section V, the computation load of existing algorithms is still high. Hence, a low-complexity algorithm should be developed.

To the best of our knowledge, there has been no research that emphasizes on the design of UT receiver in SM DL MU-MIMO system. In this work, we consider the PSM scheme and apply the generalized spatial modulation (GSM) proposed in [16], [25] in DL MU-MIMO system. BSTx antennas are separated into K groups corresponding to K UTs and each UT is equipped with N_r receiving antennas. At each group, GSM is employed by activating a subset of antennas simultaneously for data transmission. Specifically, rather than the ZF precoder, we aim to design a blind yet low-complexity UT receiver that can jointly identify active antennas at the corresponding group of BSTx and mitigate MUI using only a small subset of CSI. The minimum-output-energy (MOE) UT receiver is developed based on the minimum power distortionlessly response (MPDR) beamforming concept as proposed in [26]. A two-stages detection process is proposed: In the pre-processing stage, a method termed as minimax is proposed to identify the indices of active antennas at each group of BSTx antennas, where the key idea is that the minimum output energy of the detector is maximized. The antenna indices that have been identified are demapped to spatial symbol and the associated CSI is sent to the post-processing stage. A constrained MOE algorithm is proposed in the post-processing stage to mitigate MUI and extract temporal symbols. Compared with existing precoding-based algorithms, the complexity is significantly reduced. Moreover, the proposed algorithm is semi-blind in which only a small subset of CSI is required to identify active antennas as well as eliminate MUI. Performance metrics including the correct identification probability and the overall symbol error rate (SER) are analyzed. Simulation results verify that the proposed scheme has attractive near-far resistant characteristics. In summary, the contributions of this work are as follows:

1) As will be discussed in Section IV, significant throughput (bits per channel use (bpcu)) enhancement of GSM scheme can be obtained compared with the conventional SM or even the QSM schemes.

2) Compared with existing precoding-based works, the proposed algorithm is more practical since only a small subset of CSI (rather than full CSI) is required.

3) As will be seen in Table 1 analyzed in Section V, the complexity of the proposed scheme is extensively reduced compared with typical existing algorithms.

4) We formulate identification of active antennas' indices into a minimax problem and the proposed MOE receiver work reliably in near-far secnario.

The rest of this paper is arranged as follows. In Section II, we introduce the signal, system as well as channel models. Section III describes and analyzes the proposed MOE-based UT receiver in DL MU MIMO SM system. Section IV further extends the algorithm in Section III to the GSM scheme. In Section V, we demonstrate the system performance and discuss the numerical results. Concluding remarks are finally made in Section VI.

Table 1 Computation load comparison of the proposed and existing algorithms

Algorithms	Number of floating-point operations
BD precoding + ML detection algorithm in [22]	$K\left(8N_{\text{tot}}N_r + N_{\text{tot}}^3 + 8N_r^2\left(M + N_{\text{tot}}\right) + 7MN_r\right)$
Proposed MOE-based two-steps detection algorithm	$K\left(8JN_r^2 + 8N_t\left(N_r^2 + N_r\right) + 8N_r\right)$
ZF Precoding (RSM) + ML detection algorithm in [14]	$KMN_r + 16(KN_r)^2N_{\text{tot}} + (KN_r)^2$

Notation: The upper and lower case boldface letters denote matrix and vector, respectively. $[\,]^{\mathrm{T}}$ and $[\,]^{\mathrm{H}}$ stand for matrix or vector transpose and complex transpose, respectively. $\|\boldsymbol{a}\|$ denotes the l_2–norm of vector $\boldsymbol{a}$. We use $E\{\}$ indicates ensemble average, and $\equiv$ for "is defined as". $\boldsymbol{I}_K$ denotes an identity matrix of size K. $\boldsymbol{e}_k^L$ denotes the kth column vector of an identity matrix of size L. A complex normal random variable with mean μ variance σ^2 reads as $CN\left(\mu,\sigma^2\right)$. $\hat{x}$ means the estimate of x. $\boldsymbol{A}(i,j)$ denotes the element of the ith row and jth column of matrix $\boldsymbol{A}$. $\lfloor x\rfloor$ is the floor function that rounds x down, and returns the largest integer that is less than or equal to x. $\left(\begin{smallmatrix} M \\ L \end{smallmatrix}\right) = \frac{M!}{L!(M-L)!}$, $M \geq L$ denotes the combination of L out of M.

II. System Model and Problem Formulation

We consider a single-cell SM DL MU-MIMO system in which a BSTx with N_{tot} transmitting antennas communicates with K UTs simultaneously. A schematic illustration of the system is depicted in Figure 1. As shown in Figure 1, the N_{tot} transmitting antennas are uniformly separated into K groups, and each group corresponds to a single user. We assume that $N_{\text{tot}} = KN_t$, $N_t = 2^n$, n is a positive integer. Each UT is equipped with N_r receiving antennas, thereby, a $N_t \times N_r$ MIMO system is dedicated for each user.

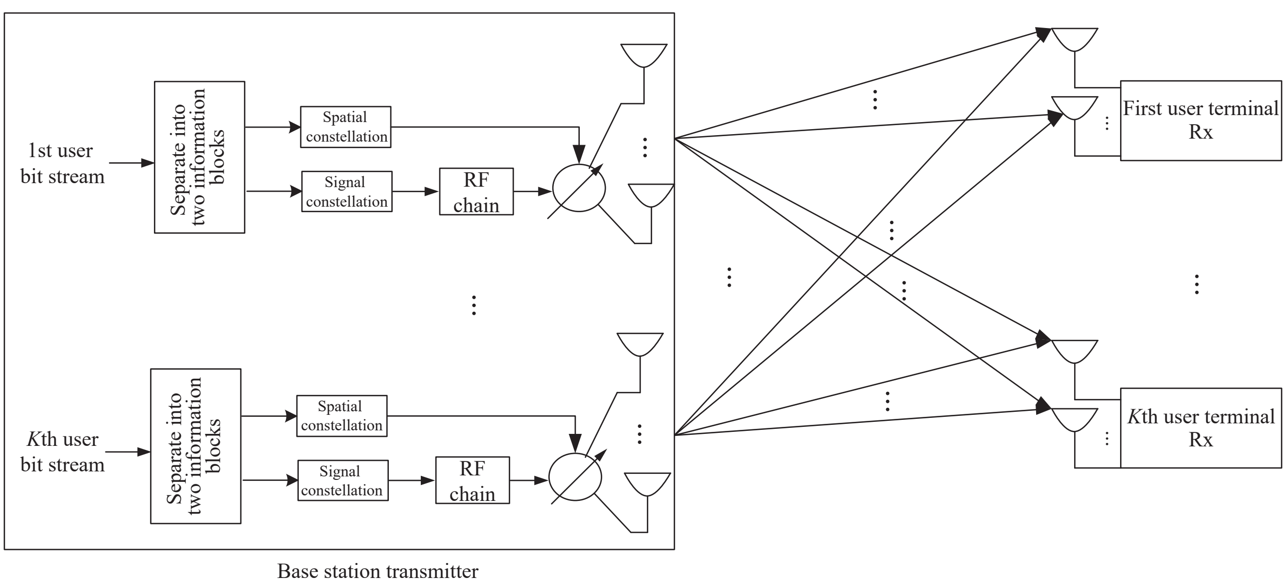

Figure 1 Block diagram of the downlink SM multiuser MIMO system.

In SM scheme, the bit stream intended for kth UT is composed of two blocks at any transmission time interval: the first block contains n bits denoted as $\left[\begin{array}{cccc} b_1^k & b_2^k & \cdots & b_n^k \end{array}\right]$, which are used to activate a particular antenna at the kth group. The second block contains m bits denoted as $\left[\begin{array}{cccc} b_{n+1}^k & b_{n+2}^k & \cdots & b_{n+m}^k \end{array}\right]$, which are mapped to a specific symbol in the conventional signal constellation diagram with size $M = 2^m$. Therefore, a symbol interval, T_s, is equal to

$$T_s = T_{s1} + T_{s2} = (n+m)\,T_b = \left(\log_2 N_t + \log_2 M\right)T_b \quad (1)$$

where T_b is the bit duration.

Let $\left\{\boldsymbol{h}_{i,j}^k\right\}_{\substack{k,i=1,2,\ldots,K\\ j=1,2,\ldots,N_t}} \in C^{N_r\times 1}$ be the instantaneous channel vector as seen by the kth UT's array of antennas from the jth antenna in the ith group of BSTx. In this paper, Rayleigh fading channel is assumed, without the consideration of path loss or shadowing effect, i.e., any entry in $\left\{\boldsymbol{h}_{i,j}^k\right\}_{\substack{k,i=1,2,\ldots,K\\ j=1,2,\ldots,N_t}}$ is distributed as $CN(0,1)$. The channel parameters are totally uncorrelated (independent). We may combine $\left\{\boldsymbol{h}_{i,j}^k\right\}_{\substack{k,i=1,2,\ldots,K\\ j=1,2,\ldots,N_t}}$ and express the channel parameters between the ith group of BSTx and kth UT as $\boldsymbol{H}_i^k \equiv \left[\begin{array}{cccc} \boldsymbol{h}_{i,1}^k & \boldsymbol{h}_{i,2}^k & \cdots & \boldsymbol{h}_{i,N_t}^k \end{array}\right]$

$\in \mathbb{C}^{N_r \times N_t}$, then the overall channel parameters can be expressed as

$$\boldsymbol{H} = \begin{bmatrix} \boldsymbol{H}_1^1 & \boldsymbol{H}_2^1 & \cdots & \boldsymbol{H}_K^1 \\ \boldsymbol{H}_1^2 & \boldsymbol{H}_2^2 & \cdots & \boldsymbol{H}_K^2 \\ \cdots & \cdots & \ddots & \cdots \\ \boldsymbol{H}_1^K & \boldsymbol{H}_2^K & \cdots & \boldsymbol{H}_K^K \end{bmatrix}_{KN_r \times KN_t} \tag{2}$$

The submatrix in the diagonal of matrix $\boldsymbol{H}$, i.e., $\{\boldsymbol{H}_k^k\}_{k=1,2,\ldots,K}$, is referred to as intended MIMO channel, while the off-diagonal matrices, i.e., $\{\boldsymbol{H}_i^k\}_{i \neq k}$, are the interference MIMO channels. In this paper, we invoke the assumption that the kth UT has only the intended MIMO CSI, i.e., $\{\boldsymbol{h}_{i,j}^k\}_{\substack{k,i=1,2,\ldots,K \\ j=1,2,\ldots,N_t}}$ or $\boldsymbol{H}_k^k$, but has no knowledge of the CSIs of all interference MIMO channels, $\{\boldsymbol{H}_i^k\}_{\substack{i\neq k \\ i=1,2,\ldots}}$. In practical scenario, $\boldsymbol{H}_k^k$ can be acquired or estimated by periodically sending delta-like pilot signals from the kth group transmit antennas of BSTx that propagate to the kth UT. Then, the kth UT can acquire the channel impulse response (CIR).

III. Design of MOE-Based UT Receiver in Downlink Multiuser SM System

1. Algorithm description

For analytical tractability, we first deal with the case that only single antenna for each group at BSTx is activated during one symbol interval. Extension to the GSM scheme will be analyzed in the next section. The received vector at the kth UT's array of antennas during the $i$ith symbol interval can be written as

$$\begin{aligned} \boldsymbol{r}_k(i) &= \sum_{k'=1}^{K} \sqrt{P_{k'}} \boldsymbol{h}_{k',j_{k'}}^k s_{k'}(i) + \boldsymbol{v}_k(i) \\ &= \sqrt{P_k} \boldsymbol{h}_{k,j_k}^k s_k(i) + \sum_{\substack{k'=1 \\ k'\neq k}}^{K} \sqrt{P_{k'}} \boldsymbol{h}_{k',j_{k'}}^k s_{k'}(i) + \boldsymbol{v}_k(i) \\ &= \sqrt{P_k} \boldsymbol{h}_{k,j_k}^k s_k(i) + \boldsymbol{u}_k(i) \end{aligned} \tag{3}$$

where $j_{k'}$ denotes the index of activated transmit antenna in the k'th group of antennas at BSTx, $j_{k'} \in \{1,2,\ldots,N_t\}$, $k' \in \{1,2,\ldots,K\}$, and $\boldsymbol{r}_k(i), \boldsymbol{v}_k(i) \in C^{N_r \times 1}$. $\boldsymbol{v}_k(i)$ denotes AWGN vector received by kth UT. The elements of the noise vector are assumed to be i.i.d. complex Gaussian random variables with zero mean and variance σ^2, i.e. $\boldsymbol{v}_k(i) \sim CN(\boldsymbol{0}, \sigma^2 \boldsymbol{I}_{N_r})$. $P_{k'}$ is the received power for the k'th UT. $\{S_{k'}(i)\}_{\substack{k'=1,2,\ldots,K \\ i=1,2,\ldots}}$ is the ith modulated temporal symbol for k'th UT and is selected with equal a priori probability from the conventional M-ary PSK signal constellation $\aleph$. We assume that the average power of the PSK signal carried by each user is normalized to one, $E\{|s_{k'}(i)|^2\} = 1$. The first term on the right hand side of (3) is the desired signal and $\boldsymbol{u}_k(i) \equiv \sum_{\substack{k'=1 \\ k'\neq k}}^{K} \sqrt{P_{k'}} \boldsymbol{h}_{k',k_k}^k s_{k'}(i) + \boldsymbol{v}_k(i)$ represents the MUI plus background noise term. To decode the spatial and temporal data designated for kth UT, we aim to estimate j_k as well as extract $s_k(i)$ from the observation vector $\boldsymbol{r}_k(i)$.

The optimum decision rule is realized to satisfy the maximum-likelihood (ML) criterion. Under AWGN, the ML algorithm is equivalent to minimize the Euclidean distance between the received vector and the signal vector. Based on (3), the active antenna index of the kth group at the BSTx and the corresponding data symbol carried by it could be detected as

$$\left[\hat{j}_{k,\mathrm{ML}}, \hat{s}_{k,\mathrm{ML}}(i)\right] = \arg \min_{\substack{\{j_{k'}\}_{k'=1,2,\ldots,K} \in \{1,2,\ldots,N_t\} \\ \{s_{k'}(i)\}_{k'=1,2,\ldots,K} \in \{1,2,\ldots,M\}}} \left\| \boldsymbol{r}_k(i) - \sum_{k'=1}^{K} \sqrt{P_{k'}} \boldsymbol{h}_{k',j_{k'}}^k s_{k'}(i) \right\|^2 \tag{4}$$

The detection procedure needs exhaustive searches throughout all possible antenna indices of each group as well as all possible M-ary temporal symbols. It is inapplicable to the proposed scheme for the reasons below:

1) To implement the ML detection, the kth UT should have all the CSIs, i.e., $\boldsymbol{H}$. However, as we have described in Section II, only the intended MIMO CSI, $\boldsymbol{H}_k^k$ is available.

2) Even though in the SM case, (4) needs to be evaluated by $(N_t M)^K$ times. The load of computation expands dramatically with a growth rate of $(N_t M)$. The complexity is intensive and prohibitive since it requires to jointly optimize all the parameters, let alone the GSM case.

Therefore, employing only the partial CSI, $\boldsymbol{H}_k^k$, we develop a linear MOE-based UT receiver in DL SM MU-MIMO system. The illustrative diagram of the MOE-based detector is presented in Figure 2.

To recover the desired symbol, $s_k(i)$, an N_r-by-1 weight vector $\boldsymbol{w}_k$ is designed to combine the information collected from all received antennas of kth UT.

$$y_k(i) = \boldsymbol{w}_k^{\mathrm{H}} \boldsymbol{r}_k(i) = \sqrt{P_k} \boldsymbol{w}_k^{\mathrm{H}} \boldsymbol{h}_{k,j_k}^k s_k(i) + \boldsymbol{w}_k^{\mathrm{H}} \boldsymbol{u}_k(i) \tag{5}$$

The temporal symbol is then demodulated by applying the minimum distance (MD) decision rule.

$$\hat{s}_k(i) = Q(y_k(i)) \tag{6}$$

where $Q(\cdot)$ is the demodulation function.

The rationale of the proposed MOE receiver is analogous to the MPDR beamformer in [26] that is widely applied in array signal processing. If $\boldsymbol{h}_{k,j_k}^k$ has been perfectly estimated, the choice of $\boldsymbol{w}_k$ to meet the MOE criterion is to minimize the output energy, while maintain

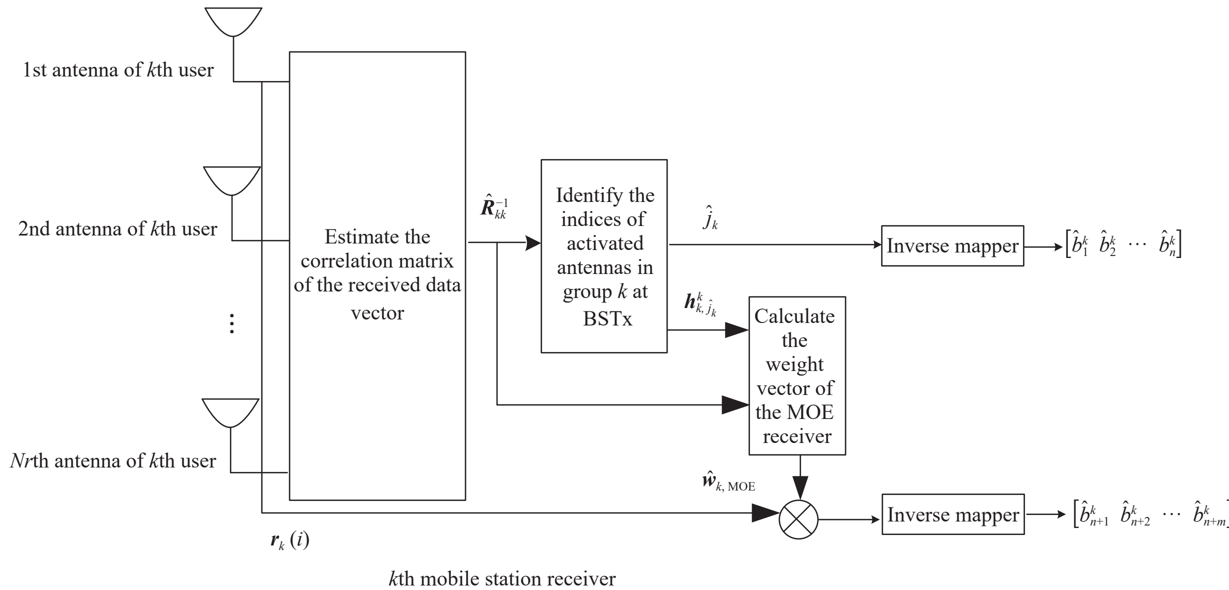

Figure 2 Schematic diagram of the kth user's MOE-based SM receiver.

the deaired signal distortionlessly. This yields

$$\boldsymbol{w}_{k,\mathrm{MOE}} = \left\{ \begin{array}{c} \arg\min\limits_{\boldsymbol{w}_k} E\left\{\left|\boldsymbol{w}_k^{\mathrm{H}}\boldsymbol{r}_k\left(i\right)\right|^2\right\} \\ \text{s.t.} \quad \boldsymbol{w}_k^{\mathrm{H}}\boldsymbol{h}_{k,j_k}^k = 1 \end{array} \right\} \tag{7}$$

The mean output energy can be calculated as

$$\begin{aligned} E\left\{\left|\boldsymbol{w}_k^{\mathrm{H}}\boldsymbol{r}_k\left(i\right)\right|^2\right\} &= E\left\{\boldsymbol{w}_k^{\mathrm{H}}\boldsymbol{r}_k\left(i\right)\boldsymbol{r}_k^{\mathrm{H}}\left(i\right)\boldsymbol{w}_k\right\} \\ &= \boldsymbol{w}_k^{\mathrm{H}} E\left\{\boldsymbol{r}_k\left(i\right)\boldsymbol{r}_k^{\mathrm{H}}\left(i\right)\right\}\boldsymbol{w}_k \\ &= \boldsymbol{w}_k^{\mathrm{H}}\boldsymbol{R}_{kk}\boldsymbol{w}_k \end{aligned} \tag{8}$$

where $\boldsymbol{R}_{kk} = E\left\{\boldsymbol{r}_k\left(i\right)\boldsymbol{r}_k^{\mathrm{H}}\left(i\right)\right\}$ is the correlation matrix of the observation vector $\boldsymbol{r}_k\left(i\right)$. Using Lagrange multiplier to solve the constrained optimization problem, we can obtain the solution of (7) as

$$\boldsymbol{w}_{k,\mathrm{MOE}} = \lambda_k \boldsymbol{R}_{kk}^{-1}\boldsymbol{h}_{k,j_k}^k = \frac{\boldsymbol{R}_{kk}^{-1}\boldsymbol{h}_{k,j_k}^k}{\left(\boldsymbol{h}_{k,j_k}^k\right)^{\mathrm{H}}\boldsymbol{R}_{kk}^{-1}\boldsymbol{h}_{k,j_k}^k} \tag{9}$$

where $\lambda_k = \boldsymbol{w}_{k,\mathrm{MOE}}^{\mathrm{H}}\boldsymbol{R}_{kk}\boldsymbol{w}_{k,\mathrm{MOE}} = \frac{1}{\left(\boldsymbol{h}_{k,j_k}^k\right)^{\mathrm{H}}\boldsymbol{R}_{kk}^{-1}\boldsymbol{h}_{k,j_k}^k}$ is the mean output energy of the MOE receiver. Therefore, the output of the MOE receiver can be obtained as

$$\begin{aligned} y_k\left(i\right) &= \boldsymbol{w}_{k,\mathrm{MOE}}^{\mathrm{H}}\boldsymbol{r}_k\left(i\right) \\ &= \boldsymbol{w}_{k,\mathrm{MOE}}^{\mathrm{H}}\sum_{k'=1}^{K}\sqrt{P_{k'}}\boldsymbol{h}_{k',j_{k'}}^k s_{k'}\left(i\right) + \boldsymbol{w}_{k,\mathrm{MOE}}^{\mathrm{H}}\boldsymbol{v}_k\left(i\right) \\ &= \sqrt{P_k}\boldsymbol{w}_{k,\mathrm{MOE}}^{\mathrm{H}}\boldsymbol{h}_{k,j_k}^k s_k\left(i\right) \\ &\quad + \boldsymbol{w}_{k,\mathrm{MOE}}^{\mathrm{H}}\left(\sum_{\substack{k'=1 \\ k'\neq k}}^{K}\sqrt{P_{k'}}\boldsymbol{h}_{k',j_k}^k s_{k'}(i) + \boldsymbol{v}_k(i)\right) \\ &= \sqrt{P_k}s_k\left(i\right) + \boldsymbol{w}_{k,\mathrm{MOE}}^{\mathrm{H}}\boldsymbol{u}_k\left(i\right) \end{aligned} \tag{10}$$

In what follows, the signal to interference plus noise ratio (SINR) of the kth MOE receiver, denoted as γ_k, can be calculated as

$$\begin{aligned} \gamma_k &= \frac{E\left\{\left|\boldsymbol{w}_{k,\mathrm{MOE}}^{\mathrm{H}}\sqrt{P_k}\boldsymbol{h}_{k,j_k}^k s_k\left(i\right)\right|^2\right\}}{E\left\{\left|\boldsymbol{w}_{k,\mathrm{MOE}}^{\mathrm{H}}\boldsymbol{u}_k\left(i\right)\right|^2\right\}} \\ &= \frac{P_k\boldsymbol{w}_{k,\mathrm{MOE}}^{\mathrm{H}}\boldsymbol{h}_{k,j_k}^k E\left\{\left|s_k\left(i\right)\right|^2\right\}\left(\boldsymbol{h}_{k,j_k}^k\right)^{\mathrm{H}}\boldsymbol{w}_{k,\mathrm{MOE}}}{\boldsymbol{w}_{k,\mathrm{MOE}}^{\mathrm{H}}E\left\{\boldsymbol{u}_k\left(i\right)\boldsymbol{u}_k^{\mathrm{H}}\left(i\right)\right\}\boldsymbol{w}_{k,\mathrm{MOE}}} \\ &= \frac{P_k}{\boldsymbol{w}_{k,\mathrm{MOE}}^{\mathrm{H}}\boldsymbol{R}_{uu}\boldsymbol{w}_{k,\mathrm{MOE}}} \\ &= \frac{P_k}{\lambda_k - P_k} \end{aligned} \tag{11}$$

where $\boldsymbol{R}_{uu} \equiv E\left\{\boldsymbol{u}_k\left(i\right)\boldsymbol{u}_k^{\mathrm{H}}\left(i\right)\right\}$ is the correlation matrix of the interference plus noise. In deriving (11), we have use the identity that

$$\begin{aligned} \boldsymbol{R}_{uu} &\equiv E\Bigg\{\left(\boldsymbol{r}_k\left(i\right) - \sqrt{P_k}\boldsymbol{h}_{k,j_k}^k s_k\left(i\right)\right) \\ &\qquad \cdot\left(\boldsymbol{r}_k\left(i\right) - \sqrt{P_k}\boldsymbol{h}_{k,j_k}^k s_k\left(i\right)\right)^{\mathrm{H}}\Bigg\} \\ &= \boldsymbol{R}_{kk} - P_k\boldsymbol{h}_{k,j_k}^k\left(\boldsymbol{h}_{k,j_k}^k\right)^{\mathrm{H}} \end{aligned} \tag{12}$$

An alternative representation of γ_k, which is derived in the Appendix A, is

$$\gamma_k = P_k\left(\boldsymbol{h}_{k,j_k}^k\right)^{\mathrm{H}}\boldsymbol{R}_{uu}^{-1}\boldsymbol{h}_{k,j_k}^k \tag{13}$$

Please note that the solution of MOE receiver also maximizes the output SINR since it essentially minimizes the output energy while preserves the desired signal distortionlessly. As depicted in (9), the MOE receiver requires accurate information of $\boldsymbol{h}_{k,j_k}^k$, since otherwise, mismatch or pointing error ($\hat{j}_k \neq j_k$ induced $\boldsymbol{h}_{k,\hat{j}_k}^k \neq \boldsymbol{h}_{k,j_k}^k$) will severely degrade system's performance. In next subsection, we develop a simple yet efficient algorithm to estimate j_k.

2. Detection of $\{j_k\}_{k=1,2,\ldots,K}$ by Minimax method

The rationale of the proposed minimax method relies on the fact that accurate $\boldsymbol{h}_{k,j_k}^k$ maximizes the mean output energy of the MOE receiver. We first note that the mean output energy of the MOE receiver as derived in Section III.1 is given by

$$\begin{aligned}\lambda_k &= \boldsymbol{w}_{k,\mathrm{MOE}}^{\mathrm{H}} \boldsymbol{R}_{kk} \boldsymbol{w}_{k,\mathrm{MOE}} \\ &= P_k \left| \boldsymbol{w}_{k,\mathrm{MOE}}^{\mathrm{H}} \boldsymbol{h}_{k,j_k}^k \right|^2 + \boldsymbol{w}_{k,\mathrm{MOE}}^{\mathrm{H}} \boldsymbol{R}_{uu} \boldsymbol{w}_{k,\mathrm{MOE}} \\ &= P_k + \boldsymbol{w}_{k,\mathrm{MOE}}^{\mathrm{H}} \boldsymbol{R}_{uu} \boldsymbol{w}_{k,\mathrm{MOE}} \end{aligned} \tag{14}$$

As depicted in (14), the mean output energy of the MOE receiver is composed of two parts: The first part is the power of the desired user, P_k, since it has been distortionlessly passed according to the constraint depicted in (7). While the second part is the residual energies, $\boldsymbol{w}_{k,\mathrm{MOE}}^{\mathrm{H}} \boldsymbol{R}_{uu} \boldsymbol{w}_{k,\mathrm{MOE}}$, arisen from the interferers and background noise that have been suppressed to meet the criterion in (7).

Therefore, we can claim that, λ_k is dominated by P_k. That is, λ_k should be slightly larger than the desired signal's energy. However, if the idle antenna is erroneously identified as the active one, i.e., $\hat{j}_k \neq j_k$, which results in the deviation of the desired user's spatial signature vector from the actual one, $\boldsymbol{h}_{k,\hat{j}_k}^k \neq \boldsymbol{h}_{k,j_k}^k$. This may induce disastrous effect since the MOE receiver attempts to mitigate any user with spatial signature vector different from $\boldsymbol{h}_{k,\hat{j}_k}^k$ in order to minimize the output energy. Toward this end, the desired user will be misregarded as another interferer that is apt to be suppressed by the MOE receiver. Consequently, the output energy degrades in accordance with the estimation error. Motivated by the estimation error induced output energy reduction, we propose to estimate $\boldsymbol{h}_{k,j_k}^k$ such that the minimum output energy is maximized. We refer it as "minimax" method.

Based on the rationale described above, we first create the spatial energy spectrum as

$$f\left(\boldsymbol{h}_{k,l}^k\right) = \frac{1}{\left(\boldsymbol{h}_{k,l}^k\right)^{\mathrm{H}} \boldsymbol{R}_{kk}^{-1} \boldsymbol{h}_{k,l}^k} \tag{15}$$

Substituting the well-known channel vectors between kth group antennas of BSTx and kth UT, $\left\{\boldsymbol{h}_{k,l}^k\right\}_{l=1,2,\ldots,N_t}$, into (15), then the active antenna index can be estimated by choosing the largest one among $\left\{f\left(\boldsymbol{h}_{k,l}^k\right)\right\}_{l=1,2,\ldots,N_t}$.

$$\hat{j}_k = \arg \max_{l \in \{1,2,\ldots,N_t\}} f\left(\boldsymbol{h}_{k,l}^k\right) \tag{16}$$

The estimated active antenna index, $\hat{j}_k$, is then decoded to the spatial symbol, $\{b_1^k \quad b_2^k \quad \cdots \quad b_n^k\}_{k=1,2,\ldots,K}$. At the same time, $\boldsymbol{h}_{k,\hat{j}_k}^k$ is employed by the MOE receiver for temporal symbol detection.

However, practically $\boldsymbol{R}_{kk}$ requires to be estimated. Assume stationary and ergodic random process, the ensemble average can be replaced by performing time-average on the observations, $\{\boldsymbol{r}_k(i)\}_{i=1,2,\ldots}$. Thus, during observation length (window size) of J time slots, the estimate of $\boldsymbol{R}_{kk}$ is given by

$$\hat{\boldsymbol{R}}_{kk} = \frac{1}{J} \sum_{i=1}^{J} \boldsymbol{r}_k(i) \boldsymbol{r}_k^{\mathrm{H}}(i) \tag{17}$$

As depicted in (17), in this paper, we estimate the correlation matrix of the received vector by performing J-duration time average. Nevertheless, there exists inevitable estimation error, which is arisen from finite window size. It can be further reduced as we use larger window size.

In a nutshell, the proposed algorithm implemented at the kth UT is as following:

Step 1 Collecting J data vectors $\{\boldsymbol{r}_k(i)\}_{i=1,2,\ldots,J}$, and applying (17) to compute $\hat{\boldsymbol{R}}_{kk}$.

Step 2 Using $\hat{\boldsymbol{R}}_{kk}$ obtained in Step 1 to create the energy spectrum

$$f\left(\boldsymbol{h}_{k,l}^k\right) = \frac{1}{\left(\boldsymbol{h}_{k,l}^k\right)^{\mathrm{H}} \hat{\boldsymbol{R}}_{kk}^{-1} \boldsymbol{h}_{k,l}^k}, \quad l = 1,2,\ldots,N_t \tag{18}$$

Step 3 Using (18) to estimate the activated transmit antenna of kth group at the BSTx.

$$\hat{j}_k = \arg \max_{l \in \{1,2,\ldots,N_t\}} f\left(\boldsymbol{h}_{k,l}^k\right), \quad k = 1,2,\ldots,K$$

Step 4 Using $\boldsymbol{h}_{k,\hat{j}_k}^k$ obtained in Step 3 to calculate $\hat{\boldsymbol{w}}_{k,\mathrm{MOE}}$ of the MOE receiver using (9).

$$\hat{\boldsymbol{w}}_{k,\mathrm{MOE}} = \frac{\hat{\boldsymbol{R}}_{kk}^{-1} \boldsymbol{h}_{k,\hat{j}_k}^k}{\left(\boldsymbol{h}_{k,\hat{j}_k}^k\right)^{\mathrm{H}} \hat{\boldsymbol{R}}_{kk}^{-1} \boldsymbol{h}_{k,\hat{j}_k}^k} \tag{19}$$

Step 5 Using the result acquired in Step 4 to obtain the temporal symbol estimate.

$$\hat{s}_k(i) = Q\left(\hat{\boldsymbol{w}}_{k,\mathrm{MOE}}^{\mathrm{H}} \boldsymbol{r}_k(i)\right)$$

Step 6 De-mapping $\hat{j}_k$ to $\left[\ \hat{b}_1^k \quad \hat{b}_2^k \quad \cdots \quad \hat{b}_n^k\ \right]$.

Step 7 De-mapping $\hat{s}_k(i)$ to $\left[\ \hat{b}_{n+1}^k \quad \hat{b}_{n+2}^k \quad \cdots \quad \hat{b}_{n+m}^k\ \right]$.

The schematic diagram of the kth UT's MOE-based SM receiver is shown in Figure 2.

IV. Design of MOE-Based UT Receiver in GSM DL MU-MIMO

The proposed algorithm is flexible, in which it can be easily extended from SM to GSM scheme. If D out of N_t at each group of transmit antennas of the BSTx are activated simultaneously, the spectral efficiency (bpcu) can be extensively increased. In other words, as D=1, GSM reduces to SM. Moreover, the bpcu can be further enhanced by multiplexing the temporals sent by the activated antennas. Specifically, D temporal symbols can be carried at the same time slot by different activated transmitting antenna in each group of BSTx.

Compared to the SM scheme described in Section III, GSM increases bpcu from $K\times(\lfloor\log_2 N_t\rfloor+\log_2 M)$ to $K\times\left(\left\lfloor\log_2\left(\begin{array}{c}N_t\\D\end{array}\right)\right\rfloor+D\times\log_2 M\right)$. It has been validated in the work of [27] that the bpcu increases as we increase D. This demonstrates that the bpcu is dramatically improved by employing GSM.

For notational simplicity, we assume the first D antennas for each group are activated in the proceeding analysis, though extension to any set of D antennas is without conceptual difficulty. We denote the symbols dedicated to the kth UT carried by the D active antennas as $\{s_{k,1}(i)\quad s_{k,2}(i)\quad\cdots\quad s_{k,D}(i)\}_{\substack{k=1,2,\ldots,k\\ i=1,2,\ldots}}$, respectively. To extract the D symbols, a bank of D MOE receivers should be implemented at each UT. Please note that in addition to MUI and background noise as described in the previous section, the intersymbol interference (ISI) for the GSM scheme should also be mitigated. The received signal by the kth UT's array of antennas during the ith symbol interval can be written as

$$\begin{aligned}\boldsymbol{r}_k(i)&=\sum_{k'=1}^{K}\sum_{l=1}^{D}\sqrt{P_{k'}}\boldsymbol{h}_{k',l}^{k}s_{k',l}(i)+\boldsymbol{v}_k(i)\\&=\sqrt{P_k}\boldsymbol{h}_{k,j}^{k}s_{k,j}(i)+\sqrt{P_k}\sum_{\substack{l=1\\l\neq j}}^{D}\boldsymbol{h}_{k,l}^{k}s_{k,l}(i)\\&\quad+\sum_{\substack{k'=1\\l\neq k}}^{K}\sum_{l=1}^{D}\sqrt{P_{k'}}\boldsymbol{h}_{k',l}^{k}s_{k',l}(i)+\boldsymbol{v}_k(i)\\&=\sqrt{P_k}\boldsymbol{h}_{k,j}^{k}s_{k,j}(i)+\sqrt{P_k}\sum_{\substack{l=1\\l\neq j}}^{D}\boldsymbol{h}_{k,l}^{k}s_{k,l}(i)+\boldsymbol{u}_k(i)\end{aligned}\tag{20}$$

where l denotes the activated transmit antenna index in each group of antennas at BSTx. We assume that $s_{k,j}(i)$ is the desired symbol, then as depicted in (20), ISI is the sum of $(D-1)$ terms. $\boldsymbol{u}_k(i)$ represents the MUI plus background noise term. The proposed UT receiver in DL MU-MIMO GSM system is inherently a two-step process: At the front-end of kth UT receiver, the D indices of active antennas at the kth group of BSTx should be estimated and then decoded into spatial information bits, $\left[\begin{array}{cccc}b_1^k & b_2^k & \cdots & b_n^k\end{array}\right]$. In the second step, the estimated CSIs are exploited to develop a bank of D linear receivers that can jointly suppress ISI, MUI, as well as background noise. The outputs of the D linear receivers at kth UT can be written, respectively, as

$$\begin{aligned}y_{k,j}(i)&=\boldsymbol{w}_{k,j}^{\mathrm{H}}\boldsymbol{r}_k(i)\\&=\sqrt{P_k}\boldsymbol{w}_{k,j}^{\mathrm{H}}\boldsymbol{h}_{k,j}^{k}s_{k,j}(i)\\&\quad+\sqrt{P_k}\boldsymbol{w}_{k,j}^{\mathrm{H}}\sum_{\substack{l=1\\l\neq j}}^{D}\boldsymbol{h}_{k,l}^{k}s_{k,l}(i)+\boldsymbol{w}_{k,j}^{\mathrm{H}}\boldsymbol{u}_k(i)\end{aligned}\tag{21}$$

where $\{\boldsymbol{w}_{k,j}\}_{j=1,2,\ldots,D}$ denotes the N_r-by-1 weight vector designed to extract the symbol of $\{s_{k,j}(i)\}_{j=1,2,\ldots,D}$, respectively. And $\hat{s}_{k,j}(i)=Q(y_{k,j}(i))$. If the active antennas have been perfectly estimated, we propose to design the jth receiver at the kth UT to meet the MOE criterion subject to multiple constraints, yielding

$$\boldsymbol{w}_{k,j,\mathrm{MOE}}=\left\{\begin{array}{l}\arg\min\limits_{\boldsymbol{w}_{k,j}}E\left\{\left|\boldsymbol{w}_{k,j}^{\mathrm{H}}\boldsymbol{r}_k(i)\right|^2\right\}=\boldsymbol{w}_{k,j}^{\mathrm{H}}\boldsymbol{R}_{kk}\boldsymbol{w}_{k,j}\\ \text{s.t.}\left\{\begin{array}{l}\boldsymbol{w}_{k,j}^{\mathrm{H}}\boldsymbol{h}_{k,j}^{k}=1\\ \boldsymbol{w}_{k,j}^{\mathrm{H}}\boldsymbol{h}_{\substack{k,l\\l\neq j}}^{k}=0,\ l=1,2,\ldots,D\end{array}\right.\end{array}\right.\tag{22}$$

In writing the constraints of formular (22), we have exploited the available CSIs obtained in step 1 to remove ISI. Upon defining the N_r by D constraint matrix $\boldsymbol{H}_{k,D}^{k}\equiv\left[\begin{array}{ccccc}\boldsymbol{h}_{k,1}^{k}&\cdots&\boldsymbol{h}_{k,j}^{k}&\cdots&\boldsymbol{h}_{k,D}^{k}\end{array}\right]_{N_r\times D}$, we may convert (22) into a more concise form

$$\boldsymbol{w}_{k,j,\mathrm{MOE}}=\left\{\begin{array}{c}\arg\min\limits_{\boldsymbol{w}_{k,j}}\boldsymbol{w}_{k,j}^{\mathrm{H}}\boldsymbol{R}_{kk}\boldsymbol{w}_{k,j}\\ \text{s.t.}\left(\boldsymbol{H}_{k,D}^{k}\right)^{\mathrm{H}}\boldsymbol{w}_{k,j}=\boldsymbol{e}_j^{D}\end{array}\right\}\tag{23}$$

where $\boldsymbol{e}_j^D$ is the jth column vector of the identity matrix $\boldsymbol{I}_D$. Using Lagrange multiplier method, it is able to convert (23) into unconstrained optimization problem. The solution of (23) can be obtained as

$$\begin{aligned}\boldsymbol{w}_{k,j,\mathrm{MOE}}&=\boldsymbol{R}_{kk}^{-1}\boldsymbol{H}_{k,D}^{k}\left[\left(\boldsymbol{H}_{k,D}^{k}\right)^{\mathrm{H}}\boldsymbol{R}_{kk}^{-1}\boldsymbol{H}_{k,D}^{k}\right]^{-1}\boldsymbol{e}_j^{D},\\&\quad j=1,2,\ldots,D\end{aligned}\tag{24}$$

In what follows, the output of the jth MOE receiver of kth UT leads to

$$\begin{aligned}y_{k,j}(i)&=\boldsymbol{w}_{k,j,\mathrm{MOE}}^{\mathrm{H}}\boldsymbol{r}_k(i)\\&=\sqrt{P_k}\boldsymbol{w}_{k,j,\mathrm{MOE}}^{\mathrm{H}}\boldsymbol{h}_{k,j}^{k}s_{k,j}(i)\\&\quad+\sqrt{P_k}\boldsymbol{w}_{k,j,\mathrm{MOE}}^{\mathrm{H}}\sum_{\substack{l=1\\l\neq j}}^{D}\boldsymbol{h}_{k,l}^{k}s_{k,l}(i)+\boldsymbol{w}_{k,j,\mathrm{MOE}}^{\mathrm{H}}\boldsymbol{u}_k(i)\\&=\sqrt{P_k}s_{k,j}(i)+\boldsymbol{w}_{k,j,\mathrm{MOE}}^{\mathrm{H}}\boldsymbol{u}_k(i)\end{aligned}\tag{25}$$

In deriving (25), we have implicitly apply the constraints of (23). The SINR of the proposed jth MOE receiver can then be calculated from (25) as

$$\begin{aligned}\gamma_{k,j} &= \frac{E\left\{\left|\boldsymbol{w}_{k,j,\mathrm{MOE}}^{\mathrm{H}}\sqrt{P_k}\boldsymbol{h}_{k,j}^{k}s_{k,j}\left(i\right)\right|^2\right\}}{E\left\{\left|\boldsymbol{w}_{k,j,\mathrm{MOE}}^{\mathrm{H}}\boldsymbol{u}_k\left(i\right)\right|^2\right\}}\\ &= \frac{P_k}{\boldsymbol{w}_{k,j,\mathrm{MOE}}^{\mathrm{H}}\boldsymbol{R}_{uu}\boldsymbol{w}_{k,j,\mathrm{MOE}}}\\ &= \frac{P_k}{\lambda_{k,j}-P_k}\end{aligned} \tag{26}$$

where the mean output energy of the jth MOE receiver can be derived as

$$\begin{aligned}\lambda_{k,j} &= E\left\{\left|\boldsymbol{w}_{k,j,\mathrm{MOE}}^{\mathrm{H}}\boldsymbol{r}_k\left(i\right)\right|^2\right\}\\ &= \boldsymbol{w}_{k,j,\mathrm{MOE}}^{\mathrm{H}}\boldsymbol{R}_{kk}\boldsymbol{w}_{k,j,\mathrm{MOE}}\\ &= \left[\left(\boldsymbol{H}_{k,D}^{k}\right)^{\mathrm{H}}\boldsymbol{R}_{kk}^{-1}\boldsymbol{H}_{k,D}^{k}\right]^{-1}\left(j,j\right),\\ & j=1,2,\ldots,D\end{aligned} \tag{27}$$

Define the N_r by D matrix $\boldsymbol{W}_{k,\mathrm{MOE}} \equiv \boldsymbol{R}_{kk}^{-1}\boldsymbol{H}_{k,D}^{k} \cdot \left[\left(\boldsymbol{H}_{k,D}^{k}\right)^{\mathrm{H}}\boldsymbol{R}_{kk}^{-1}\boldsymbol{H}_{k,D}^{k}\right]^{-1}$, then $\left\{\boldsymbol{w}_{k,j,\mathrm{MOE}}\right\}_{j=1,2,\ldots,D}$ is the jth column vector of $\boldsymbol{W}_{k,\mathrm{MOE}}$. Thereby, the output of D MOE receivers of kth UT yields

$$\begin{aligned}\boldsymbol{y}_k\left(i\right) &= \boldsymbol{W}_{k,\mathrm{MOE}}^{\mathrm{H}}\boldsymbol{r}_k\left(i\right)\\ &= \sqrt{P_k}\boldsymbol{W}_{k,\mathrm{MOE}}^{\mathrm{H}}\sum_{l=1}^{D}\boldsymbol{h}_{k,l}^{k}s_{k,l}\left(i\right)+\boldsymbol{W}_{k,\mathrm{MOE}}^{\mathrm{H}}\boldsymbol{u}_k\left(i\right)\\ &= \sqrt{P_k}\boldsymbol{W}_{k,\mathrm{MOE}}^{\mathrm{H}}\boldsymbol{H}_{k,D}^{k}\boldsymbol{s}_k\left(i\right)+\boldsymbol{W}_{k,\mathrm{MOE}}^{\mathrm{H}}\boldsymbol{u}_k\left(i\right)\\ &= \sqrt{P_k}\boldsymbol{s}_k\left(i\right)+\boldsymbol{W}_{k,\mathrm{MOE}}^{\mathrm{H}}\boldsymbol{u}_k\left(i\right)\end{aligned} \tag{28}$$

where $\boldsymbol{y}_k\left(i\right), \boldsymbol{s}_k\left(i\right) \in C^{D\times 1}, \boldsymbol{y}_k\left(i\right) \equiv \left[y_{k,1}\left(i\right) \quad y_{k,2}\left(i\right) \quad \cdots \quad y_{k,D}\left(i\right)\right]^{\mathrm{T}}$, $\boldsymbol{s}_k\left(i\right) \equiv \left[s_{k,1}\left(i\right) \quad s_{k,2}\left(i\right) \quad \cdots \quad s_{k,D}\left(i\right)\right]^{\mathrm{T}}$. It should be noted that to implement the MOE receiver, accurate information of $\boldsymbol{H}_{k,D}^{k}$ is required. Moreover, the indices of the active transmit antennas in the kth group carries spatial information bits, $\left[b_1^k \quad b_2^k \quad \cdots \quad b_n^k\right]$. Similar to the Minimax method proposed in Section III.2, we first construct the spatial energy spectrum function

$$f\left(\boldsymbol{h}_{k,l}^{k}\right) = \frac{1}{\left(\boldsymbol{h}_{k,l}^{k}\right)^{\mathrm{H}}\boldsymbol{R}_{kk}^{-1}\boldsymbol{h}_{k,l}^{k}},\ l=1,2,\ldots,N_t$$

In GSM scheme, there are D antennas in each group of BSTx being activated simultaneously. Hence, we choose among the set $\{f(\boldsymbol{h}_{k,1}^{k}), f(\boldsymbol{h}_{k,2}^{k}), \ldots, f(\boldsymbol{h}_{k,N_t}^{k})\}$ the D largest (peaks) values to obtain the active antenna indices' estimate. In summary, the detection and estimation algorithm of the MOE-based UT receiver in GSM DL MU-MIMO system is:

Step 1 Collecting J data vectors $\{\boldsymbol{r}_k\left(i\right)\}_{i=1,2,\ldots,J}$, and applying (17) to compute $\hat{\boldsymbol{R}}_{kk}$.

Step 2 Using $\hat{\boldsymbol{R}}_{kk}$ obtained in Step 1 to create the energy spectrum as depicted in (18).

Step 3 Choosing among the set $\{f(\boldsymbol{h}_{k,1}^{k}), f(\boldsymbol{h}_{k,2}^{k}), \ldots, f(\boldsymbol{h}_{k,N_t}^{k})\}$ the D largest values to obtain the active antenna indices' estimate.

Step 4 Using $\hat{\boldsymbol{H}}_{k,D}^{k}$ obtained in Step 3 to calculate the weight vectors of the MOE receiver.

$$\hat{\boldsymbol{W}}_{k,\mathrm{MOE}} = \hat{\boldsymbol{R}}_{kk}^{-1}\hat{\boldsymbol{H}}_{k,D}^{k}\left[\left(\hat{\boldsymbol{H}}_{k,D}^{k}\right)^{\mathrm{H}}\hat{\boldsymbol{R}}_{kk}^{-1}\hat{\boldsymbol{H}}_{k,D}^{k}\right]^{-1} \tag{29}$$

Step 5 Using the result acquired in Step 4 to obtain the spatial symbols' estimate.

$$\hat{\boldsymbol{s}}_k\left(i\right) = Q\left(\hat{\boldsymbol{W}}_{k,\mathrm{MOE}}\boldsymbol{r}_k\left(i\right)\right)$$

Step 6 De-mapping $\left\{\ \hat{j}_1 \quad \hat{j}_2 \quad \cdots \quad \hat{j}_D\ \right\}$ to the spatial information bits $\left[\ \hat{b}_1^k \quad \hat{b}_2^k \quad \cdots \quad \hat{b}_n^k\ \right]$.

Step 7 De-mapping $\{\hat{s}_{k,l}\left(i\right)\}_{l=1,2,\ldots,D}$ to the temporal information bits $\left\{\left[\ \hat{b}_{n+1}^{k,l} \quad \hat{b}_{n+2}^{k,l} \quad \cdots \quad \hat{b}_{n+m}^{k,l}\ \right]\right\}_{l=1,2,\ldots,D}$.

V. Performance Evaluation

1. Complexity analysis

In this subsection, we attempt to analyze and compare the computation load of the proposed MOE-based scheme with ZF precoding-based RSM scheme proposed in [14] and BD precoding-based EQSM scheme proposed in [22]. The complexity measurement uses the total number of floating-point operations (flops) in [28] required in both transmission and reception. For real additions and multiplications, one flop is carried out, while complex additions and multiplications require two and six flops, respectively. Hence, multiplication of $m \times n$ and $n \times p$ complex matrices needs $8mnp$ flops.

The number of flops required to implement the proposed MOE-based, BD precoding+single-user ML detection, and ZF precoding+single-user ML detection algorithms are summarized in Table 1. Please note that the flops of $8JN_r^2, 8N_t\left(N_r^2+N_r\right), 8N_r$ in the second row of Table 1, arises from the correlation matrix estimation, identification of active antenna's index, and linear detector, respectively. Taking the parameters' setting $J=40$, $K=10$, $N_{\mathrm{tot}}=80$, $n_T=n_R=8$, and $M=16$ as a working example, the number of complex multiplications required for the proposed MOE-based, BD Precoding + single-user ML detection, and ZF Precoding (RSM scheme) + single-user ML detection algorithms are respectively 251,520, 5,671,680 and 8,199,680. It is shown that the complexity of the proposed algorithm is extensively simplified compared to the existing two algorithms.

2. SER analysis

In this subsection, computer simulations are conducted to evaluate the performances of the proposed MOE-based UT receiver in DL MU-MIMO system. Unless otherwise mentioned, the number of transmit antennas in each group of BSTx and the number of UTs are set as $N_t = 10, K = 3$, respectively, for all the simulations. We define the parameter of desired user's signal-to-noise ratio for evaluation as

$$\mathrm{SNR}_k \equiv 10\log_{10}\frac{P_k}{\sigma^2}\,(\mathrm{dB}) \tag{30}$$

In the first simulation example, we attempt to evaluate the proposed MOE-based active antennas' identification algorithm. In the SM case, Figure 3 reveals the active antenna's correct identification probability, i.e., $P^k_{\text{ant correct}} = P(\hat{j}_k = j_k)$, versus the number of antennas at UT (N_r), where we set each UT's SNR to be 10 dB and N_r varies from 8 to 35. Please note that the simulation results are resulted from the successful rate of 10,000 independent tests. The window size used to estimate the correlation matrix, $\hat{\boldsymbol{R}}_{kk}$, is set to be 30, 50, 70, respectively, in order for comparison. As depicted in Figure 3, $P^k_{\text{ant correct}}$ increases as N_r increases, and it approaches 1 (perfect identification) as N_r>14. Moreover, Figure 3 verifies that larger J leads to higher $P^k_{\text{ant correct}}$. This can be expected since as J increases, the estimation error of the correlation matrix reduces. And accurate correlation matrix is essential for the MOE-based algorithm. To evaluate the capability of the proposed algorithm to survive in the near-far environment, we aim to evaluate the performance by fixing the SNR of the desired user and increasing the power of all the remaining users. We first define the near-far ratio (NFR) as

$$\mathrm{NFR} \equiv 10\log_{10}\frac{P_{\text{undesired users}}}{P_{\text{desired user}}}\,(\mathrm{dB}) \tag{31}$$

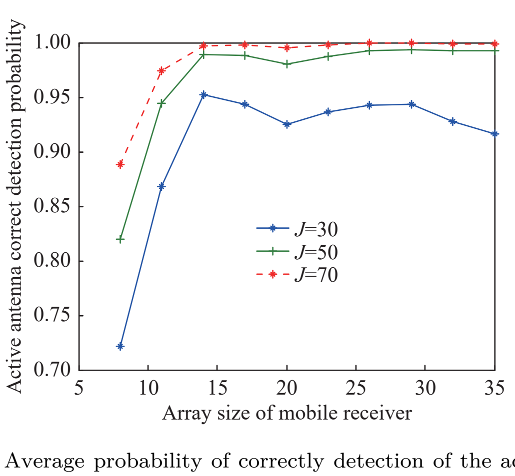

Figure 3 Average probability of correctly detection of the activated antenna versus the UT array size (N_r) in SM scheme.

Figure 4 presents $P^k_{\text{ant correct}}$ versus the NFR, where $N_r = 30$ and the desired user's SNR is 6 dB. NFR varies from 0.5 to 10 dB. As depicted in Figure 4, $P^k_{\text{ant correct}}$ is insensitive to different values of NFR. It reveals that the proposed minimax algorithm is reliabl in near-far situation. The results also verifies that higher J yields better performance. Figure 5 presents $P^k_{\text{ant correct}}$ versus SNR, where the cases for single (SM), 2 and 3 (GSM) activated antennas are evaluated for comparison. Note that in GSM, $P^k_{\text{ant correct}} = P(\hat{j}_{k,1} = j_{k,1}, \hat{j}_{k,2} = j_{k,2}, \ldots, \hat{j}_{k,D} = j_{k,D})$, that is, identification succeeds if and only if all the activated antennas are correctly detected. As we vary all the UTs' SNR from 1 dB to 12 dB, it is as expected that $P^k_{\text{ant correct}}$ increases in accordance with SNR. We can also verify from Figure 5 that smaller number of activated antennas corresponds to higher $P^k_{\text{ant correct}}$.

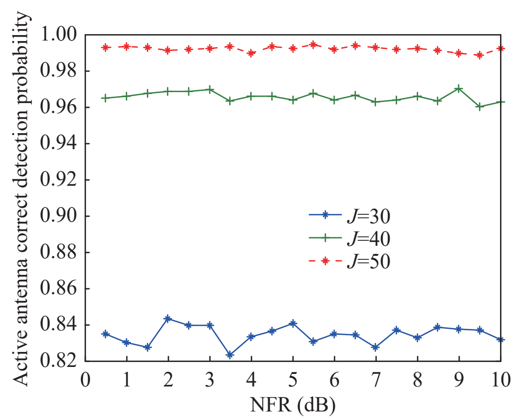

Figure 4 Average probability of correctly detection of the activated antenna versus the near-far ratio (NFR) in SM scheme.

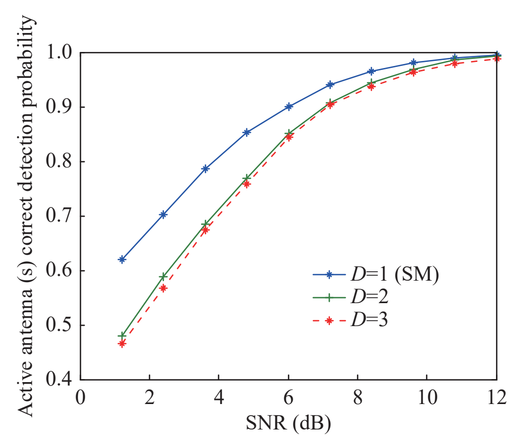

Figure 5 Average probability of correctly detection of the activated antenna(s) with respect to SNR in GSM scheme.

In the following simulations, we aim to measure the overall symbol (including spatial and temporal symbols) decoding error probability. It is quite complicated to analyze the overall SER for the SM or GSM scheme, hence, we adopt the upper bound SER as derived in [29].

$$P^k_{\text{overall error}} \leq \left(1 - P^k_{\text{ant correct}}\right) + P^k_{\text{symbol error|ant correct}}\, P^k_{\text{ant correct}} \tag{32}$$

We employ (32) as a performance metric to evaluate the proposed MOE-based algorithm, where $P^k_{\text{ant correct}}$ is obtained from the successful rate of 10000 independent trials. The performance of the ZF-precoding based SM scheme (analytical results in [14, Eqs.(26) and (27)]) is also provided for comparison. In the simulation parameters setup, we consider 3 UT ($K=3$), each equipped with $N_r=20$ receiving antennas, the number of BSTx antennas is $N_{\text{tot}}=60$, QPSK modulation formats. Figure 6 presents overall SER bound versus SNR (ranges from 6 to 15 dB) in which the proposed MOE scheme for SM and GSM (2 and 3 activated antennas, respectively) as well as the ZF-precoding based SM scheme are provided for comparison. Each curve in Figure 6 is averaged over all UTs. Since the ZF-precoding scheme in [14] are applied only in SM (only single antenna is activated), we focus the comparison only on the SM scheme for fairly comparison. As depicted in Figure 6, the ZF-precoding scheme outperforms the proposed MOE-based algorithm. However, lower complexity and more flexibility (without the limitation of $N_{\text{tot}} \geq KN_r$ and only partial CSI is required) of the proposed algorithm overwhelms slightly degradation in SER performance in comparison with the ZF-precoding scheme. We can also observe from Figure 6 that SM outperforms the GSM scheme especially when SNR is large. This may arise from the fact that more effort has been placed to mitigate ISI and MUI for the GSM scheme such that the resulted SINR at the output of MOE receiver is decreased. The near-far resistant capability of the proposed MOE receiver is verified in Figure 7, where we fix the desired user's SNR 10 dB and the NFR values vary from 1 to 10 dB. In the last simulation example, overall SER bound with respect to the N_r is presented, where the desired user's SNR = 12dB. As revealed in Figure 8, SER performance is improved as N_r increases, since larger N_r corresponds to higher degrees-of-freedom for the MOE receiver to suppress ISI as well as MUI.

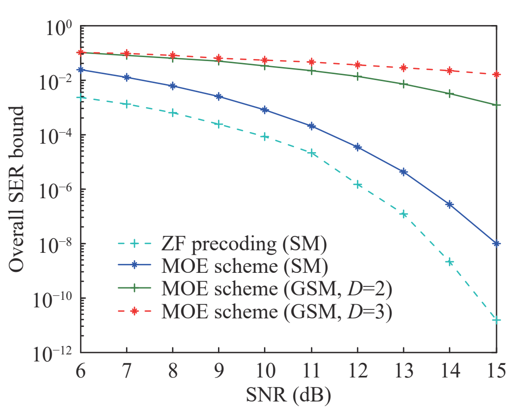

Figure 6 Overall SER versus SNR of the proposed MOE scheme for SM and GSM (2 and 3 activated antennas, respectively) as well as the ZF-precoding based SM scheme.

VI. Conclusions

In this paper, we have proposed a novel joint identification and signal detection scheme in downlink GSM MU-MIMO system. Based on the MOE criterion, the active antennas at the related group of BSTx are first identified, and the information is then utilized to perform interference suppression and temporal data extraction.

Through theoretical analysis and computer simulations, we have demonstrated that the proposed scheme can identify the activated antennas with high correct detection probability. Moreover, we have verified in Figure 4 and Figure 7 that both the identification and detection algorithm work reliably in near-far environment. As a whole, the proposed MOE-based UT receiver is blind (only a small subset of CSI is required), simple (linear processing of the received data vector) yet reliable, is suitable to be applied in current and future networks.

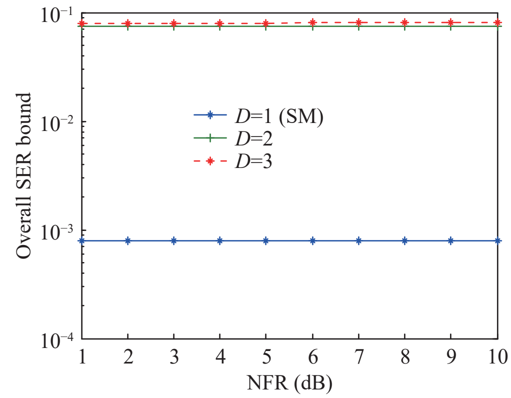

Figure 7 Overall SER bound with respect to NFR in GSM scheme.

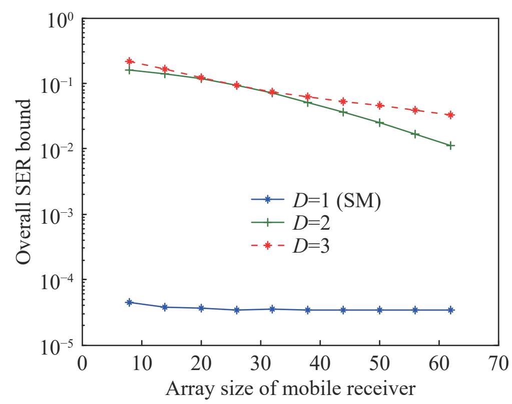

Figure 8 Overall SER bound versus the UT array size (N_r).

Appendix A. Derivation of Equation (13)

Applying Woodbury's identity in [26], we have

$$\begin{aligned}\boldsymbol{R}_{kk}^{-1} &= \left(P_k \boldsymbol{h}_{k,j_k}^k \left(\boldsymbol{h}_{k,j_k}^k\right)^{\mathrm{H}} + \boldsymbol{R}_{uu}\right)^{-1} \\ &= \boldsymbol{R}_{uu}^{-1} - \frac{P_k}{1 + P_k \left(\boldsymbol{h}_{k,j_k}^k\right)^{\mathrm{H}} \boldsymbol{R}_{uu}^{-1} \boldsymbol{h}_{k,j_k}^k} \boldsymbol{R}_{uu}^{-1} \boldsymbol{h}_{k,j_k}^k \left(\boldsymbol{h}_{k,j_k}^k\right)^{\mathrm{H}} \boldsymbol{R}_{uu}^{-1}\end{aligned} \tag{A-1}$$

Substituting (A-1) into the mean output energy of the MOE receiver, we arrive at

$$\lambda_k = \frac{1}{\left(\boldsymbol{h}_{k,j_k}^k\right)^{\mathrm{H}}\boldsymbol{R}_{kk}^{-1}\boldsymbol{h}_{k,j_k}^k} = \frac{1}{\left(\boldsymbol{h}_{k,j_k}^k\right)^{\mathrm{H}}\left[\boldsymbol{R}_{uu}^{-1} - \frac{P_k}{1+P_k\left(\boldsymbol{h}_{k,j_k}^k\right)^{\mathrm{H}}\boldsymbol{R}_{uu}^{-1}\boldsymbol{h}_{k,j_k}^k}\boldsymbol{R}_{uu}^{-1}\boldsymbol{h}_{k,j_k}^k\left(\boldsymbol{h}_{k,j_k}^k\right)^{\mathrm{H}}\boldsymbol{R}_{uu}^{-1}\right]\boldsymbol{h}_{k,j_k}^k}$$

$$= \frac{1}{\frac{\left(\boldsymbol{h}_{k,j_k}^k\right)^{\mathrm{H}}\boldsymbol{R}_{uu}^{-1}\boldsymbol{h}_{k,j_k}^k}{1+P_k\left(\boldsymbol{h}_{k,j_k}^k\right)^{\mathrm{H}}\boldsymbol{R}_{uu}^{-1}\boldsymbol{h}_{k,j_k}^k}} = \frac{1+P_k\left(\boldsymbol{h}_{k,j_k}^k\right)^{\mathrm{H}}\boldsymbol{R}_{uu}^{-1}\boldsymbol{h}_{k,j_k}^k}{\left(\boldsymbol{h}_{k,j_k}^k\right)^{\mathrm{H}}\boldsymbol{R}_{uu}^{-1}\boldsymbol{h}_{k,j_k}^k} \tag{A-2}$$

Substituting (A-2) into (11), yields

$$\gamma_k = \frac{P_k}{\lambda_k - P_k} = \frac{P_k}{\frac{1+P_k\left(\boldsymbol{h}_{k,j_k}^k\right)^{\mathrm{H}}\boldsymbol{R}_{uu}^{-1}\boldsymbol{h}_{k,j_k}^k}{\left(\boldsymbol{h}_{k,j_k}^k\right)^{\mathrm{H}}\boldsymbol{R}_{uu}^{-1}\boldsymbol{h}_{k,j_k}^k} - P_k}$$

$$= P_k\left(\boldsymbol{h}_{k,j_k}^k\right)^{\mathrm{H}}\boldsymbol{R}_{uu}^{-1}\boldsymbol{h}_{k,j_k}^k \tag{A-3}$$

which gives (13).

References

[1] E. Basar, M. W. Wen, R. Mesleh, *et al.*, "Index modulation techniques for next-generation wireless networks," *IEEE Access*, vol. 5, pp. 16693–16749, 2017.

[2] R. Y. Mesleh, H. Haas, S. Sinanovic, *et al.*, "Spatial modulation," *IEEE Transactions on Vehicular Technology*, vol. 57, no. 4, pp. 2228–2241, 2008.

[3] R. Mesleh, H. Haas, C. W. Ahn, *et al.*, "Spatial modulation—A new low complexity spectral efficiency enhancing technique," in *Proceedings of the 1st International Conference on Communications and Networking in China*, Beijing, China, pp.1–5, 2006.

[4] M. Di Renzo, H. Haas, and P. M. Grant, "Spatial modulation for multiple-antenna wireless systems: a survey," *IEEE Communications Magazine*, vol. 49, no. 12, pp. 182–191, 2011.

[5] M. W. Wen, B. X. Zheng, K. J. Kim, *et al.*, "A survey on spatial modulation in emerging wireless systems: research progresses and applications," *IEEE Journal on Selected Areas in Communications*, vol. 37, no. 9, pp. 1949–1972, 2019.

[6] S. M. Song, Y. L. Yang, Q. Xion, *et al.*, "A channel hopping technique I: theoretical studies on band efficiency and capacity," in *Proceedings of 2004 International Conference on Communications, Circuits and Systems*, Chengdu, China, pp.229–233, 2004.

[7] J. Jeganathan, A. Ghrayeb, L. Szczecinski, *et al.*, "Space shift keying modulation for MIMO channels," *IEEE Transactions on Wireless Communications*, vol. 8, no. 7, pp. 3692–3703, 2009.

[8] M. X. Zhang, W. W. Miao, Y. T. Shen, *et al.*, "Joint spatial modulation and beamforming based on statistical channel state information for hybrid massive MIMO communication systems," *IET Communications*, vol. 13, no. 10, pp. 1458–1464, 2019.

[9] N. Serafimovski, S. Sinanovixć, A. Younis, *et al.*, "2-User multiple access spatial modulation," in *Proceedings of the 6th IEEE International Workshop on Heterogeneous, Multi-Hop, Wireless and Mobile Networks*, Houston, TX, USA, pp.343–347, 2011.

[10] T. L. Narasimhan, P. Raviteja, and A. Chockalingam, "Large-scale multiuser SM-MIMO versus massive MIMO," in *Proceedings of 2014 Information Theory and Applications Workshop (ITA)*, San Diego, CA, USA, pp.1–9, 2014.

[11] J. P. Zheng, "Low-complexity detector for spatial modulation multiple access channels with a large number of receive antennas," *IEEE Communications Letters*, vol. 18, no. 11, pp. 2055–2058, 2014.

[12] W. L. Zhang, "SAGE based data detection for multiuser spatial modulation with large number of receive antennas," *IEEE Communications Letters*, vol. 19, no. 9, pp. 1520–1523, 2015.

[13] E. Z. Zhou and L. Hao, "On the detection of multiple-access spatial modulations," *Chinese Journal of Electronics*, vol. 26, no. 1, pp. 172–178, 2017.

[14] K. M. Humadi, A. I. Sulyman, and A. Alsanie, "Spatial modulation concept for massive multiuser MIMO systems," *International Journal of Antennas and Propagation*, vol. 2014, article no. 563273, 2014.

[15] A. Stavridis, M. Di Renzo, P. M. Grant, *et al.*, "On the asymptotic performance of receive space modulation in the shadowing broadcast channel," *IEEE Communications Letters*, vol. 20, no. 10, pp. 2103–2106, 2016.

[16] R. Pizzio, B. F. Uchôa-Filho, M. D. Renzo, *et al.*, "Generalized spatial modulation for downlink multiuser MIMO systems with multicast," in *2016 IEEE 27th Annual International Symposium on Personal, Indoor, and Mobile Radio Communications*, Valencia, Spain, pp.1–6, 2016.

[17] A. Stavridis, M. D. Renzo, and H. Haas, "Performance analysis of multistream receive spatial modulation in the MIMO broadcast channel," *IEEE Transactions on Wireless Communications*, vol. 15, no. 3, pp. 1808–1820, 2016.

[18] S. Narayanan, M. J. Chaudhry, A. Stavridis, *et al.*, "Multiuser spatial modulation MIMO," in *Proceedings of 2014 IEEE Wireless Communications and Networking Conference*, Istanbul, Turkey, pp.671–676, 2014.

[19] X. P. Wu, M. Di Renzo, and H. Haas, "A novel multiple access scheme based on spatial modulation MIMO," in *2014 IEEE 19th International Workshop on Computer Aided Modeling and Design of Communication Links and Networks (CAMAD)*, Athens, Greece, pp.285–289, 2014.

[20] M. Maleki, H. R. Bahrami, and A. Alizadeh, "Layered spatial modulation for multiuser communications," *IEEE Transactions on Wireless Communications*, vol. 15, no. 10, pp. 7143–7159, 2016.

[21] X. R. Li, Y. Zhang, L. M. Xiao, *et al.*, "A novel precoding scheme for downlink multi-user spatial modulation system," in *2013 IEEE 24th Annual International Symposium on Personal, Indoor, and Mobile Radio Communications*, London, UK, pp.1361–1365, 2013.

[22] F. R. Castillo-Soria, C. A. Gutierrez, A. García-Barrientos, *et al.*, "EQSM-based multiuser MIMO downlink transmission for correlated fading channels," *EURASIP Journal on Wireless Communications and Networking*, vol. 2020, no. 1, article no. 30, 2020.

[23] F. R. Castillo-Soria, E. Basar, J. Cortez, *et al.*, "Quadrature spatial modulation based multiuser MIMO transmission system," *IET Communications*, vol. 14, no. 7, pp. 1147–1154, 2020.

[24] R. Zhang, L. L. Yang, and L. Hanzo, "Generalised pre-coding aided spatial modulation," *IEEE Transactions on Wireless Communications*, vol. 12, no. 11, pp. 5434–5443, 2013.

[25] J. T. Wang, S. Y. Jia, and J. Song, "Generalised spatial modulation system with multiple active transmit antennas and low complexity detection scheme," *IEEE Transactions on Wireless Communications*, vol. 11, no. 4, pp. 1605–1615, 2012.

[26] H. L. Van Trees, *Optimum Array Processing*: *Part IV of Detection, Estimation, and Modulation Theory*. John Wiley &

Sons, Inc., New York, NY, USA, 2002, doi: 10.1002/0471221104.

[27] W. C. Wu, "EVD-based multiuser detection in uplink generalized spatial modulation MIMO systems," *Arabian Journal for Science and Engineering*, vol. 47, no. 11, pp. 13811–13821, 2022.

[28] M. H. A. Khan, K. M. Cho, M. H. Lee, *et al.*, "A simple block diagonal precoding for multi-user MIMO broadcast channels," *EURASIP Journal on Wireless Communications and Networking*, vol. 2014, no. 1, article no. 95, 2014.

[29] J. T. Wang, S. Y. Jia, and J. Song, "Signal vector based detection scheme for spatial modulation," *IEEE Communications Letters*, vol. 16, no. 1, pp. 19–21, 2012.

Wei-Chiang WU received the M.S. and Ph.D. degrees both in electrical engineering from the Taiwan Tsing Hua University, Hsinchu, China, in 1992 and 1998, respectively. He has been a Professor at the Department of Electrical Engineering, Da-Yeh University, Changhua, China. He is now a Professor at the Department of College of Mechanical and Electrical Engineering, Sanming University, Sanming, China. His current research interests include multiuser MIMO detection, smart antenna technology, and spatial modulation technique.
(Email: lclunds@163.com)